

Published in final edited form as:

Clin Cancer Res. 2014 November 15; 20(22): 5672–5685. doi:10.1158/1078-0432.CCR-14-0868.

Interrogating two schedules of the AKT inhibitor MK-2206 in patients with advanced solid tumors incorporating novel pharmacodynamic and functional imaging biomarkers

Timothy A. Yap^{1,2}, Li Yan³, Amita Patnaik⁴, Nina Tunariu⁵, Andrea Biondo^{1,2}, Ivy Fearen³, Kyriakos P. Papadopoulos⁴, David Olmos^{1,2}, Richard Baird^{1,2}, Liliana Delgado³, Ernestina Tetteh³, Robert A. Beckman³, Lisa Lupinacci³, Ruth Riisnaes², Shaun Decordova², Simon P. Heaton², Karen Swales², Nandita M deSouza⁵, Martin O. Leach⁵, Michelle D. Garrett², Daniel M. Sullivan⁶, Johann S. de Bono^{1,2}, and Anthony W. Tolcher⁴

¹Drug Development Unit, The Royal Marsden NHS Foundation Trust, Sutton, Surrey, UK

²Division of Clinical Studies, The Institute of Cancer Research, Surrey, UK

³Merck & Co., Inc., Whitehouse Station, NJ, USA

⁴South Texas Accelerated Research Therapeutics, San Antonio, TX, USA

⁵CR-UK and EPSRC Cancer Imaging Centre, Division of Radiotherapy and Imaging, The Institute of Cancer Research and Royal Marsden NHS Foundation Trust, Sutton, Surrey, UK

⁶H. Lee Moffitt Cancer Center & Research Institute, Tampa, FL, USA

Abstract

Purpose—Multiple cancers harbor genetic aberrations that impact AKT signaling. MK-2206 is a potent pan-AKT inhibitor with a maximum tolerated dose (MTD) previously established at 60mg

Corresponding author: Professor Johann S de Bono, MB ChB, FRCP, MSc, PhD, FMedSci, Professor of Experimental Cancer Medicine, Drug Development Unit, Royal Marsden NHS Foundation Trust, Division of Clinical Studies, The Institute of Cancer Research, Downs Road, Sutton, Surrey SM2 5PT, United Kingdom, Tel: 44-20-8722-4302, Fax: 44-20-8642-7979, johann.de-bono@icr.ac.uk.

Author Contributions

All authors were involved in the following: 1) substantial contributions to conception and design, acquisition of data, or analysis and interpretation of data; 2) drafting of article or revising it critically for important intellectual content; 3) final approval of the version to be published; and 4) agreement to be accountable for all aspects of the work in ensuring that questions related to the accuracy or integrity of any part of the work are appropriately investigated and resolved.

Conflict of Interest Statement

J. de Bono has served as a consultant for and received research funding from Merck & Co., Inc.; T.A. Yap has received honoraria from and served as a consultant for Merck & Co., Inc.; L. Yan, I. Fearen, L. Delgado, E. Tetteh, R.A. Beckman, and L. Lupinacci are current or former employees of Merck & Co., Inc., and may hold stock or stock options in the company; A.W. Tolcher reports consulting agreements with Abbott, Abgenomics, Abraxis, Actavis, Adnexus, Ambit, Amgen, AP Pharma, Aragon Pharmaceuticals, Ariad Pharmaceuticals, Arresto, Astellas, Astex/Supergen, Bayer, Bind Biosciences, BMS Japan, Celator, Celgene, Clovis, Cougar Biotechnology, Curis, Complete Genomics, Cytomx, Daiichi Sankyo, Dendreon Corp, DeNovo, Dicerna, Eisai, Eli Lilly, EMD Serono Inc., Endo, Enzon, Everist, Exelixis, Five Prime Therapeutics Inc, Galapagos NV, Genenech, Geron Corp, GlaxoSmithKlin, HUYA Bioscience International, Inovio, Icon Clinical Research, Insert Therapeutics, Intellikine, Invivis, Janssen, Johnson & Johnson, Lilly, Merck & Co., Inc., MethylGene, Micromet, Nantworks, Nektar, Neumedicines, Novartis, OncoMed, OncoGenex, Onyx, Otsuka, Pfizer, Pharmacyclics, PPD Development LP, Prescision Health Holdings, ProNai, Regeneron Pharmaceuticals, Sanofi-Aventis, Spectrum, Sunovion, Symphogen, Triphase Accelerator Corp, Vaccinex, Veeda Oncology, and Zyngeliz; N.M. deSouza has received grants from Cancer Research UK and NIHR; M.O. Leach has received grants from Merck & Co., Inc.; R. Baird, A. Biondo, S. Decordova, M.D. Garrett, S.P. Heaton, D. Olmos, K. Papadopoulos, A. Patnaik, R. Riisnaes, D.M. Sullivan, K. Swales, and N. Tunariu have no conflicts of interest to report.

on alternate days (QOD). Due to a long half-life (60-80h), a weekly (QW) MK-2206 schedule was pursued to compare intermittent QW and continuous QOD dosing.

Experimental Design—Patients with advanced cancers were enrolled onto a QW dose-escalation phase I study to investigate the safety and pharmacokinetic-pharmacodynamic profiles of tumor and platelet-rich plasma (PRP). The QOD MTD of MK-2206 was also assessed in patients with ovarian and castration-resistant prostate cancers, and patients with advanced cancers undergoing multiparametric functional magnetic resonance imaging (MRI) studies, including dynamic contrast-enhanced MRI, diffusion-weighted imaging, magnetic resonance spectroscopy and intrinsic susceptibility-weighted MRI.

Results—Seventy-one patients were enrolled; 38 patients had 60mg MK-2206 QOD, while 33 received MK-2206 at 90mg, 135mg, 150mg, 200mg, 250mg, and 300mg QW. The QW MK-2206 MTD was established at 200mg following dose-limiting rash at 250mg and 300mg. QW dosing appeared to be similarly tolerated to QOD, with toxicities including rash, gastrointestinal symptoms, fatigue, and hyperglycemia. Significant AKT pathway blockade was observed with both continuous QOD and intermittent QW dosing of MK-2206 in serially-obtained tumor and PRP specimens. The functional imaging studies demonstrated that complex multiparametric MRI protocols may be effectively implemented in a phase I trial.

Conclusions—MK-2206 safely results in significant AKT pathway blockade in QOD and QW schedules. The intermittent dose of 200mg QW is currently used in phase II MK-2206 monotherapy and combination studies.

INTRODUCTION

The serine-threonine kinase AKT is a central component of phosphatidylinositol 3-kinase (PI3K)-AKT signaling, and is critical to cell growth, survival, and proliferation [1]. Hyperactivation of this pathway is implicated as a key driver of multiple cancers, including prostate cancer and advanced ovarian tumors [2]. Many castration resistant prostate cancers (CRPC) have genomic abnormalities along the PI3K-AKT pathway, frequently through loss of *PTEN*, which supports androgen-independent tumor growth [3, 4]. The targeting of AKT in *PTEN*-loss CRPC tumors is supported by mouse models that indicate that *AKT1* loss significantly reduces prostate cancer initiation [5]. The PI3K-AKT pathway is also frequently deranged in ovarian cancer [6]. Genetic amplification and mutation of *PIK3CA* are observed in approximately 40% and 12% of ovarian cancers, respectively [7, 8]. Similarly, AKT amplification is often encountered in ovarian cancer, although AKT mutations are rare [9, 10]. In view of this, different strategies have been developed to target AKT [2, 11].

We have previously described the development of the potent, oral, allosteric AKT inhibitor MK-2206 (Merck & Co., Inc., Whitehouse Station, NJ, USA) [12, 13]. Following the observation of preclinical antitumor activity, a Phase I dose-escalation study of MK-2206 in 33 patients with advanced solid tumors was carried out, which established the maximum tolerated dose (MTD) at 60mg on alternate days (QOD) and demonstrated that MK-2206 safely induced significant AKT pathway blockade in tumor and hair follicles, with preliminary evidence of clinical activity [14].

PD evaluation of AKT blockade involves the assessment of phosphorylation signals in normal tissue, such as the phosphorylation of pSer473 AKT and downstream substrates in platelet-rich plasma (PRP), as well as in tumor biopsies. Functional imaging can also be utilised to evaluate drug PD, including dynamic contrast-enhanced magnetic resonance imaging (DCE-MRI), diffusion weighted imaging (DWI), proton magnetic resonance spectroscopy (^1H -MRS) and intrinsic susceptibility-weighted MR (ISW-MRI) [15]. DCE-MRI is a recognized tool for the characterization of tumor angiogenesis and the quantification of drug effects on tumor vascular permeability and perfusion [16-19]. DWI is also emerging as a biomarker of tumor necrosis and/or apoptosis [20, 21]. Furthermore, ^1H -MRS can detect decreases in phosphocholine content after PI3K/AKT blockade [22, 23]. Changes in the imaging parameter for ISW-MRI (R_2^*) after chemotherapy have been described in breast cancers, but the measurement of antitumor changes has not been explored with antitumor targeted agents such as AKT inhibitors [24]. The utilization of these functional imaging techniques allows the characterization of the PD of novel molecular targeted agents in phase I studies.

The study of different schedules of molecularly targeted therapies is critical for their optimal application, but is not often done in randomized phase II trials [25]. Thus, an alternative strategy is to undertake this during the expansion phase of a phase I clinical trial. In this study, cohorts of patients with CRPC, advanced ovarian cancer, and those undergoing multiparametric MRI studies were treated with 60mg QOD of MK-2206. In view of a half-life of 60h-80h observed [14], a QW schedule of MK-2206 was also evaluated to determine the safety and maximum tolerated dose (MTD)/recommended Phase II dose (RP2D) of MK-2206, and compared with QOD dosing. In addition, electrochemiluminescence assays were utilized to quantify and compare the PD effects of MK-2206 in serial tumour and PRP specimens between both schedules of MK-2206, in parallel with pharmacokinetic (PK) studies.

PATIENTS AND METHODS

This was an open-label, dose-escalation Phase I study of continuous QOD and QW oral treatment with MK-2206, conducted at three centers (Royal Marsden NHS Foundation Trust, UK; South Texas Accelerated Research Therapeutics [START], TX; and H. Lee Moffitt Cancer Center and Research Institute, FL). The study was conducted in accordance with the Declaration of Helsinki and the International Conference on Harmonization Good Clinical Practice Guidelines and approved by relevant regulatory and independent ethics committees.

Eligibility criteria

Study inclusion criteria included written informed consent; age ≥ 18 years; patients with histologically or cytologically confirmed advanced solid tumors, who failed to respond to established therapies or for whom no proven treatments existed; Eastern Cooperative Oncology Group (ECOG) performance status [26] ≤ 1 ; previous surgery or chemotherapy ≥ 4 weeks; residual toxicity from prior treatment \leq grade (G)1; adequate bone marrow, renal, and

hepatic function; fasting serum glucose $1.1\times$ the upper limit of normal (ULN) and HbA1c 8%.

Study design

For the QOD study, MK-2206 tablets were administered at 60mg QOD in 28-day cycles to fasted patients in three different cohorts, comprising patients with advanced CRPC (n=14), ovarian cancer (n=11) and those with tumors suitable for multiparametric MRI studies (n=16). For the QW study, a two-stage design was utilized. The first stage (dose-escalation phase) followed a standard three-plus-three design. Cohorts of three to six patients were to be treated at preplanned dose levels of 90, 135, 200 and 300 mg QW; intermediate-dose cohorts were permitted. The second stage (dose confirmation) employed a modification of the toxicity probability interval method [27]. The definition of DLTs included any MK-2206-related Common Terminology Criteria for Adverse Events (CTCAE) version 3.0 [28] G4 hematological toxicity, G3 neutropenia with fever, or G3 non-hematological toxicity (except for inadequately-treated G3 nausea, vomiting, or diarrhea).

Safety

Safety assessments were conducted at baseline, days 1, 2, 7, 15, 21, 27, and 28 of cycle 1, weekly in cycle 2 and subsequently every month. All patients had a history, physical examination including full ophthalmologic assessment, electrocardiogram, 24h cardiac Holter monitoring, hematology and chemistry profiling, and urine analysis. In addition to glucose monitoring, serum c-peptide and whole blood HbA1c were measured at baseline and monthly. Adverse events (AEs) and laboratory variables were assessed using CTCAE version 3.0 [28].

PK Analyses

Plasma concentrations were analyzed by non-compartmental PK methods using WinNonLin (Scientific Consultant, Apex, NC; version 5.2.1, Pharsight, Mountain View, CA) (Supplementary methods).

Biomarker studies

PD Biomarker analyses (pSer473 AKT, pSer9 GSK3 β and pThr246 PRAS40) were undertaken on PRP and tumor, where available, using assays validated to Good Clinical Practice standards on the MesoScale Discovery (MSD[®]) technology and EnVision[™] technology platforms (Supplementary methods) [29].

Tumor response

Radiological assessment of disease status was performed at baseline and every 8 weeks, according to Response Evaluation Criteria in Solid Tumors (RECIST 1.1) [30]. Serum cancer antigen 125 (CA125) was assessed according to Gynecologic Cancer Intergroup (GCIg) criteria [31] and prostate specific antigen (PSA) according to the Prostate Cancer Working Group criteria (PCWG2) [32].

MRI Methodology

Patients were studied using a 1.5T Avanto MR Siemens system (Siemens Medical Systems, Erlangen, Germany) (Supplementary Methods). The multiparametric MRI protocol included DCE-MRI, DWI, ¹H-MRS and ISW-MRI measurements. Median parameter values analyzed included transfer constant (K^{trans}) for DCE-MRI, Apparent Diffusion Coefficient (ADC) for DWI, total choline/water (tCho/Water) ratio for ¹H-MRS, and R_2^* for ISW-MRI, respectively [18, 19, 33, 34]. Patients were scanned at 4 time points: two studies pre-treatment as part of a measurement reproducibility cohort, and two studies on MK-2206 treatment on cycle 1 day 7+/-1 and cycle 1 day 21+/-4.

RESULTS

Seventy-one patients entered this study between April 2009 and January 2011 and all were included in the safety analysis (Tables 1 and 2). Thirty-three patients received MK-2206 at escalating QW doses of 90mg (n=3), 135mg (n=5), 200mg (n=17), 300mg (n=3) and intermediate doses of 250mg (n=3) and 150mg (n=2). Thirty-eight patients received MK-2206 in three 60mg QOD MTD expansion cohorts comprising CRPC, ovarian cancer and multiparametric MRI cohorts.

Safety and tolerability

Weekly (QW) schedule dose limiting toxicities (DLTs)—Patients were enrolled into once weekly cohorts of 90mg (DLTs: 0 of 3 patients), 135mg (DLTs: 0 of 4 patients), and 200mg (DLTs: 0 of 3 patients), prior to evaluation of a 300mg cohort where DLTs of G3 rash were observed in 3 of 3 patients. An intermediate dose of 250mg QW was then explored and deemed to exceed the MTD with G3 rash observed in 2 of 3 patients. Therefore, an additional 3 patients were enrolled at 200mg QW, where G3 rash was seen in 1 of 3 patients. Since only 1 of 6 patients experienced a DLT in the 200mg cohort during the dose escalation phase, this dose level was studied in a further expansion cohort of 11 patients. Overall, in this study, 4 of 17 (23.5%) patients at 200mg QW experienced DLTs (G3 rash in 3 patients; G3 dermatitis acneiform in 1 patient). According to prespecified dose escalation/de-escalation rules, a lower intermediate dose of 150mg (G3 rash in 1 of 2 patients) was also explored. However, for administrative and non-trial related reasons, the study was terminated prior to completion of enrolment to this cohort. Overall, based on review of PK/PD and safety/tolerability data from both the QOD and QW dosing schedules, the MTD/RP2D of MK-2206 was established at 200mg QW.

No DLTs were reported in patients who received MK-2206 at 90mg or 135mg QW. Dose interruptions lasting 2 to 4 weeks were required in patients with DLTs. Two patients withdrew study consent prior to re-initiation of therapy. One patient in the 200mg dose cohort resumed therapy at the same dose, while dose reduction to the next lower dose level occurred in the remaining 7 patients. No patients discontinued study therapy directly as a result of DLTs. While DLTs fully resolved in 7 of these 10 patients within 1 to 2 weeks of onset, they resolved with sequelae of dry skin in 3 patients. No treatment-related G4-5 toxicities were observed.

Weekly (QW) schedule safety and tolerability—Overall, drug-related AEs were reported in 66.7% (22/33) of patients. The most common (10%) drug-related AEs were fatigue in 45.5% (15/33) of patients, rash in 42.4% (14/33) of patients, diarrhea and nausea in 27.3% (9/33) of patients each, vomiting in 24.2% (8/33) of patients, decreased appetite in 21.2% (7/33) of patients, stomatitis in 15.2% (5/33) of patients, and pruritus, increased alanine aminotransferase levels, and headaches in 12.1% (4/33) of patients each. The majority of these AEs were G1-2. G1 hyperglycemia was observed in 3.0% (1/33) of patients following 1 cycle of treatment with MK-2206 QW. Elevated blood glucose levels were observed in 57.6% (19/33) of patients who received MK-2206 QW. Elevations were mild and transient with onset occurring with similar frequencies during cycle 1 and subsequent cycles. Post-cycle 1 HbA1c values in all patients assessed were <7%. In 4 of 6 patients assessed, C-peptide levels increased during the first cycle of treatment (range: 65.7%-166.6%).

Three patients discontinued MK-2206 for drug-related AEs of G3 rash (n=1), G3 complete atrioventricular block (n=1), and G1 rash (n=1). Eleven of 33 patients interrupted study therapy due to drug-related AEs. Of these 11 patients, 2 patients resumed therapy at the same dose, 2 patients withdrew consent and did not resume study, and 7 patients required dose reduction to the next lower dose level. Dose interruptions of one day to 4 weeks was required prior to re-initiating study therapy.

Alternate day (QOD) schedule DLTs—DLTs occurred in 7 of 38 (18.4%) patients and included G3 rash (n=5), G3 rash and G3 stomatitis (n=1), and G3 hyperglycemia (n=1) (Supplementary Table 1). One patient discontinued study treatment due to G3 rash; this resolved within one week of stopping MK-2206. Overall, DLTs resulted in dose interruption in 6 patients. Among these 6 patients, study therapy was resumed within 1-2 weeks at the same dose of 60mg QOD (n=2), a reduced dose of 30mg QOD with subsequent dose escalation to 45mg QOD (n=2), and a reduced dose of 50mg QOD (n=1); dose interruption was followed by MK-2206 discontinuation in one patient due to disease progression. All DLTs resolved to baseline levels within 1-2 weeks of drug interruption; the DLT of G3 hyperglycemia was considered to be resolved with sequelae, as this patient with pre-existing glucose intolerance remained on metformin treatment.

Alternate day (QOD) schedule safety and tolerability—The safety and tolerability of MK-2206 in a QOD schedule have previously been described in the dose-escalation study; thirty-three patients with advanced solid tumors were treated, with G1-2 rash the most common toxicity observed [14]. Other MK-2206-associated AEs included fatigue, gastrointestinal toxicities, and hyperglycemia. The QOD expansion cohorts in this study have confirmed that MK-2206 is generally well tolerated in 38 patients at the MTD of 60mg QOD, with a similar toxicity profile to that observed during dose escalation (Supplementary Table 1) [14].

Following the first cycle of treatment, G1-2 hyperglycemia was observed in 7.9% (3/38) of patients, and G3 hyperglycemia was observed in 2.6% (1/38) of patients. While not reported as AEs, blood glucose levels were noted to be elevated in 71.1% (27/38) of patients who received MK-2206 60mg QOD. The majority of elevations were mild and transient with

onset occurring during the first cycle of therapy. Baseline and end of cycle 1 HbA1c levels were available in 76.3% (29/38) of patients, with 86.2% (25/29) of these patients demonstrating HbA1c levels of $\leq 6.5\%$ at both timepoints. In 2 patients with baseline levels $\leq 6.5\%$, end of cycle 1 values were 7.3% and 8.3%, respectively. Baseline and end of cycle 1 C-peptide levels were available in 71.1% (27/38) of patients. In 85.2% (23/27) of these patients, C-peptide levels increased during the first cycle of treatment (range: 2.7% to 495.5%).

Pharmacokinetics of MK-2206

Weekly (QW) schedule pharmacokinetics—Following administration in a QW schedule, MK-2206 was absorbed with a median time to maximum concentration (T_{max}) of 4h-6h. As gastric emptying occurs within 1h-2h, the median T_{max} of 4h-6h suggests that MK-2206 absorption probably occurs in both the small intestines and stomach. MK-2206 plasma concentrations declined in a mono-exponential manner after administration at 90mg, 135mg, 200mg, 250mg, and 300mg QW (Figure 1A). The absorption and distribution of MK-2206 are consistent with its relatively low solubility, but high permeability across physiological pH ranges.

MK-2206 plasma concentrations exhibited high inter-patient variability with percent coefficient of variations (CVs) of area under the concentration-time curve (AUC) and maximum concentration (C_{max}) ranging from 12% to 71%. AUC and C_{max} increased in a dose-proportional manner within the dose range of 90mg to 300mg QW. Given the high inter-subject variability, there was no evidence of deviation from dose proportionality (Figures 1B and 1C).

Table 3 summarizes PK parameters of MK-2206 following the first and last dose of cycle 1 QW dosing. Mean terminal elimination half-lives ($t_{1/2}$) were 71.6h, 88.9h, and 75.1h after administration of 90mg, 135mg, and 200mg doses, respectively, supporting the use of MK-2206 in QW and QOD dosing schedules. Accumulation ratio of MK-2206 expressed as the geometric mean ratios $AUC_{last\ day}:AUC_{first\ day}$ or $C_{max_{last\ day}}:C_{max_{first\ day}}$ were 1.54 and 1.33, respectively, consistent with the terminal half-life, suggesting that elimination of MK-2206 did not change after QW dosing of 200mg of MK-2206 (n=17). Accumulation ratios were slightly higher after QW dosing of 135mg MK-2206 (1.91 and 1.95, respectively); this is probably attributable to the low number of patients in the 135mg cohort (n=4).

After QW administration in cycle 1, multiple-dose PK was only evaluable in 1 patient in the 90mg, 150mg, or 250mg dose cohorts, and no patients were evaluable in the 300mg QW dose cohorts. Mean C_{max} levels after 90mg to 250mg multiple QW dose administration (153 to 245 nM) were below the mean C_{max} (365nM) of the no-observed-adverse-effect-level (NOAEL) dose in dogs, while the mean C_{max} after the first dose in the 300mg cohort (466nM) was higher than the C_{max} at the NOAEL dose in dogs. The mean 48h (trough) plasma concentrations after multiple dose administration of 90mg to 300mg QW MK-2206 exceeded the prespecified 56.8nM PK target for 70% inhibition of pAKT. After QW 90mg, 135mg, and 200mg QW dosing, the mean C_{48h} values were 79.3nM, 158nM, and 187nM, respectively.

Alternate day (QOD) schedule pharmacokinetics—The peak plasma concentrations of MK-2206 occurred at median T_{max} of 4h after administration of 60mg MK-2206 QOD in the expansion cohort and the $t_{1/2}$ was 64h, which was comparable to the PK values of patients in the dose escalation cohorts (Supplementary Table 2; Supplementary Figure 1) [14]. The accumulation ratio of MK-2206, assessed as $AUC_{last\ day}:AUC_{first\ day}$ ratio, was 3.3, consistent with its elimination $t_{1/2}$ and suggests no change in PK of MK-2206 after multiple dosing compared with a single dose. A similar accumulation ratio was observed in the dose escalation cohort [14].

Weekly (QW) versus alternate day (QOD) schedule pharmacokinetics—Systemic exposure ($AUC_{Daylast}$) of MK-2206 at the 60mg QOD schedule was comparable to exposure after the 200 mg QW schedule when normalized to the 3.3-fold difference in dose (or 3.5-fold shorter dosing interval), while C_{max} was about 2-fold higher at the 200mg QW schedule compared with the 60mg QOD schedule. The terminal elimination half-lives were similar for the QOD and QW schedules, while trough concentrations after multiple 200mg QW dosing were lower than trough concentrations after multiple 60mg QOD dosing, relieving drug exposure for periods of time during treatment with the QW schedule of MK-2206.

Pharmacodynamic biomarker analysis

Weekly (QW) schedule pharmacodynamics—The analysis of paired tumor biopsies from 5 patients receiving 200mg QW of MK-2206 (Figure 2A1) showed a significant suppression of pSer473 AKT when compared with paired pre-treatment samples. Overall, the pSer473 AKT signal decreased to 50.0% (range 37.5-60.3%; $p=0.0003$) of baseline levels on MK-2206 treatment, confirming target modulation.

The PD effects of MK-2206 treatment on pSer473 AKT ($n=11$) and pSer9 GSK3 β ($n=11$) phosphorylation at the 200mg MTD were also assessed sequentially in PRP specimens at multiple timepoints (Figure 2A2-2A3). The mean pSer473 AKT signal post-MK-2206 was 19.8% at 24h ($p<0.0001$), 30.6% at 48h ($p<0.0001$), 51.7% at 96h ($p=0.0015$) and 97.4% at 168h ($p=0.92$) of baseline levels (Figure 2A2), while mean pSer9 GSK3 β signal was 65.0% at 24h ($p<0.0001$), 82.3% at 48h ($p=0.012$), 91.4% at 96h ($p=0.56$), and 117.2% at 168h ($p=0.37$) of baseline levels (Figure 2A3).

Alternate day (QOD) schedule pharmacodynamics—Paired tumor biopsies were obtained for biomarker analysis by MSD electrochemiluminescence assays from 3 patients receiving 60mg QOD of MK-2206 (Figure 2B1). All 3 patients showed a significant suppression of pSer473 AKT when compared with paired pre-treatment samples. The mean pSer473 AKT levels decreased to 50.1% (range 45.3-56.2%; $p=0.004$) of baseline levels on MK-2206 treatment, confirming target modulation.

PD effects in PRP were also assessed serially at multiple timepoints from 29 patients receiving the MTD of 60mg QOD of MK-2206 (Figure 2B2-2B4). The pSer473 AKT signal decreased significantly to mean values of 36.3% at 3h ($p<0.0001$), 27.9% at 6h ($p<0.0001$), 44.0% at 24h ($p<0.0001$), and 70.6% at 48h ($p=0.045$) of baseline levels (Figure 2B2). Overall, pSer473 AKT levels decreased significantly by a mean of 55.3%, with maximum

inhibition at 6h post-MK-2206. This suppression was sustained significantly for 48h when the next dose of drug was given.

This inhibition of pSer473 AKT was associated with significant decreases in the phosphorylation of downstream substrates pSer9 GSK3 β to mean levels of 76.8% at 3h ($p=0.009$), 67.5% at 6h ($p=0.0051$), 102.9% at 24h ($p=0.87$), and 116.1% at 48h ($p=0.51$) of baseline levels (Figure 2B3); and pThr246 PRAS40 to mean levels of 79.8% at 3h ($p=0.005$), 79.7% at 6h ($p=0.0059$), 86.9% at 24h ($p=0.030$), and 91.4% at 48h ($p=0.42$) of baseline levels (Figure 2B4). With both pSer9 GSK3 β substrates and pThr246 PRAS40, the maximum suppression was also at 6h post-MK-2206. A single patient was removed as an outlier according to Grubbs test for outliers ($\alpha=0.01$), resulting in mean levels of 60.1% pSer473 AKT ($p=0.0004$) and 81.9% pThr246 PRAS40 ($p=0.0019$) at 48h. This confirmed the suppression of pSer473 AKT and its downstream target PRAS40 were significantly sustained to 48h in the remaining 28 patients on QOD dosing.

Functional imaging cohort

Sixteen patients were enrolled into the multiparametric MRI cohort, comprising DCE-MRI, DWI, $^1\text{H-MRS}$ and ISW-MRI scans over 4 timepoints (Supplementary Tables 3-7). Each multiparametric MRI protocol lasted 45-50 minutes per patient. Two baseline scans were undertaken at a mean period of 7.4 days apart. Thirteen patients had 2 baseline studies each and were thus included in the reproducibility analysis. Of the 16 patients enrolled into this functional imaging cohort, four did not receive MK-2206 due to clinical deterioration (Supplementary Table 3). Of these remaining 12 patients, 1 patient had a non-enhancing lesion and so DCE-MRI analysis was not conducted; 1 patient had no detectable choline and therefore $^1\text{H-MRS}$ analysis was not performed; and 5 patients had significant artefacts on ISW-MRI, and thus analysis was not undertaken. Therefore, the final evaluable imaging data sets included 11 patients for DCE-MRI, 12 patients for DWI, 11 patients for $^1\text{H-MRS}$ and 7 patients for ISW-MRI analysis (Supplementary Tables 4-7).

Overall, the extent of all MRI parameter changes following treatment were within the limits of data variability as determined by the analysis of the reproducibility cohort (Supplementary Figure 2). There was, however, a statistically significant increase in median tumor ADC in four patients on day 7. The increase in ADC was maintained in two of these patients on day 21. The baseline imaging measurements in these two patients suggested increased cellularity of the tumors with varying degrees of vascularity, prior to responding to MK-2206 treatment. In one of these patients (baseline median ADC = $100 \times 10^{-5} \text{mm}^2 \text{s}^{-1}$ and median $K^{\text{trans}} = 0.08 \text{min}^{-1}$), this response was associated with a moderate reduction in K^{trans} of 20%, and there was a marginal reduction in the size of the tumor on restaging CT imaging after 6 months of treatment (Supplementary Figure 3). In the other patient who had a more vascular tumor (baseline median ADC = $97.4 \times 10^{-5} \text{mm}^2 \text{s}^{-1}$ and median $K^{\text{trans}} = 1.14 \text{min}^{-1}$), there was a significant increase in ADC values in keeping with of areas of necrosis within the enhancing and cellular rim of the tumor, while the central necrotic area of the tumor remained unchanged. This malignant lesion was stable by RECIST measurements on the restaging CT at week 8 of treatment (Supplementary Figure 4).

Antitumor activity—The median duration of treatment for patients who received MK-2206 in a QW schedule was 8.1 weeks (range: 1.1 to 24.0 weeks), compared to 13.1 weeks (range: 8.7 to 28.0 weeks) for those in the QOD cohorts. Antitumor activity was reported in a 43-year-old female with ER/PR positive, HER2 negative metastatic breast cancer (Figure 3). Additional molecular characterization demonstrated *PIK3CA* exon 20 mutation on circulating nucleic acid analysis and low Ki67 proliferation. She had previously received cyclophosphamide, doxorubicin, and radiotherapy. Following 8 weeks of treatment with MK-2206 150mg QW, a 22% reduction in RECIST measurements of target lesions in the liver lesions, celiac axis, and para-aortic lymph nodes was noted. Post-treatment MRI demonstrated intratumoral necrosis of the liver and bone metastases. Additionally, an approximate 36% reduction in CA15-3 was observed, and the patient remained on treatment for a total of 24 weeks. Apart from this patient, two patients with CRPC had RECIST SD for >6 months (range 6.5-7.5 months).

DISCUSSION

The QOD MTD/RP2D of 60mg of MK-2206 was generally well tolerated in patients with advanced cancers, as demonstrated previously [14]. The MTD/RP2D for QW dosing of MK-2206 was established at 200mg following the observation of DLTs of rash at the 250mg and 300mg QW dose levels of MK-2206. This DLT of rash is consistent with previous reports of AKT inhibition with MK-2206 and other PI3K-AKT pathway inhibitors [14, 35, 36]. Overall, the MTD/RP2D of the QW schedule of MK-2206 appeared to be similarly tolerated to QOD dosing (Table 2; Supplementary Tables 1 and 8) [14]. The pulsatile QW dosing of MK-2206 resulted in an intermittent rather than sustained blockade of AKT and downstream substrates observed with QOD dosing, thus potentially permitting some recovery of normal cellular function.

The intermittent dosing of MK-2206 is supported by the observation of PK data demonstrating lower trough concentrations after 200mg QW dosing, in contrast to 60mg QOD dosing, relieving sustained drug pressure for periods of time during the QW schedule. PK parameters following the administration of 90mg-300mg MK-2206 QW in cycle 1 indicated no auto-induction of MK-2206 metabolizing enzymes as predicted by *in vitro* PK studies. Importantly, the terminal half-life of MK-2206 (70h-90h) is supportive of a QW dosing schedule and C_{max} values up to 250mg were below the NOAEL obtained in preclinical toxicology studies, while maintaining C_{48h} values above the clinical monotherapy PK target for 70% inhibition of pSer473 AKT. Average steady-state trough MK-2206 concentrations at doses of at least 60mg QOD, and C_{48hr} concentration of MK-2206 at doses of at least 90mg QW were on average greater than the concentrations required for 70% inhibition of pSer473 AKT in whole blood (57 nmol/L), a level identified in preclinical models as associated with antitumor activity for both continuous and intermittent dosing schedules, respectively.

In this study, significant AKT inhibition was demonstrated in paired tumor biopsies and PRP specimens with both schedules of MK-2206. To our knowledge, this is the first demonstration of the feasibility of ‘real-time’ serial PRP sampling in a phase I trial setting using quantitative electrochemiluminescence assays (MSD[®]) and ELISA assays

(EnVision™ technology platform) to monitor multiple phosphoprotein changes in response to a novel molecular therapeutic, such as MK-2206. We have previously demonstrated the use of hair follicles as a surrogate tissue for the measurement of pThr246 PRAS40 PD effects, which confirmed AKT pathway blockade with MK-2206 [14].

In addition, there were differential PD effects observed between QOD and QW dosing of MK-2206, specifically with regards to the phosphorylation levels of pSer473 AKT and downstream substrates pSer9 GSK3β and pThr246 PRAS40 in serial PRP sampling (Figure 2). For example, while continuous blockade of pSer473 AKT was observed at the QOD MTD of MK-2206, with the QW MTD there was an initial suppression of the phosphorylation signal for at least 96h, followed by partial recovery by the 168h timepoint prior to the next QW dosing timepoint. The establishment of such a pulsatile QW MTD has enabled MK-2206 to be taken forward in an intermittent rather than continuous schedule for combination studies. This schedule minimized potential MK-2206 toxicities and permitted a wider therapeutic window for the co-development of different combination regimens. This is especially critical since modest antitumor efficacy has been observed with MK-2206 monotherapy and other PI3K-AKT pathway inhibitors, although anecdotal examples of patient benefit have been observed in this and other studies (Figure 3) [14, 36-38].

MK-2206-related hyperglycemia and increased C-peptide levels were observed in most patients in both dosing schedules, consistent with PD inhibition of the AKT target and pathway [36]. These elevations in glucose were mainly mild and transient, suggesting effective homeostatic compensation with raised pancreatic insulin/C-peptide release in response to decreased glucose transport and metabolism due to AKT inhibition [36]. Although the exact mechanism of MK-2206-induced hyperglycemia has not been fully elucidated, blockade of the PI3K pathway with other similar small molecule targeted inhibitors appears to be associated with peripheral insulin resistance, increased gluconeogenesis, and/or hepatic glycogenolysis [39].

The modest antitumor effects observed in this study with MK-2206 was despite statistically significant AKT blockade demonstrated in tumor and normal tissue at the MTD of both schedules of MK-2206. Nevertheless, signaling through pSer9 GSK3β and pThr246 PRAS40 was less robustly suppressed, suggesting that effective downstream AKT pathway inhibition and biological effect was not achieved (Figure 2). The lack of RECIST antitumor responses may also potentially be due to the episodic recovery of AKT pathway signaling during MK-2206 treatment as suggested by the PRP PD data (Figure 2). Such pulsatile normalization of phosphorylated protein signals towards baseline levels may nevertheless be important for the transient return of normal cellular functions and minimization of MK-2206-related toxicities. Ultimately, it will be important to define the extent and duration of target and signaling pathway inhibition required for optimal antitumor benefit and an acceptable therapeutic window.

Furthermore, the limited antitumor activity observed may be due to signalling pathway crosstalk and/or disruption of feedback loops following the administration of MK-2206 monotherapy, justifying the development of this drug in molecularly-defined patient populations and in combination studies with other antitumor agents [25, 40]. It is therefore

likely that the future development of AKT inhibitors will involve combination strategies with targeted agents against other rational targets including MEK, ER, AR, and the proteasome, as well as chemotherapies for the treatment of solid tumors. The use of an intermittent schedule of MK-2206 may improve tolerability and widen the therapeutic window of combination regimens. The pulsatile dosing of MK-2206 will also permit a higher degree, albeit shorter duration, of target blockade, which may potentially minimize tumor cell adaptation and eventual secondary drug resistance [25].

MK-2206 has now been assessed in combination with the MEK inhibitor selumetinib (AstraZeneca; AZD6244) in patients with advanced solid tumors, including those with RAS mutant cancers [41]. Critically, the pulsatile QW schedule of MK-2206 improved the tolerability of this combination compared with continuous QOD dosing and enabled a RP2D to be established. Importantly, objective antitumor responses were observed in those with advanced *KRAS* mutant non-small cell lung carcinoma and ovarian cancers following treatment with this novel drug combination.

The functional imaging study demonstrated for the first time that a combined DCE-MRI, DWI, ISW-MRI & ¹H-MRS protocol may be implemented effectively in a phase I trial within a reasonable scanning time of 45-50min. The imaging protocol used in our studies also successfully combined DCE-MRI, DWI, and ISW-MRI data acquisition in the same plane through the same tumor volume, permitting the use of a common ROI across the different modalities included. Such an approach not only potentially reduces the time required for data analysis, but also offers the opportunity to explore tumor heterogeneity using a multiparameter analysis and multi-segmentation approach. In our studies, the reproducibility measured was better with the DWI parameter (<10%) in contrast to DCE-MRI, ¹H-MRS and ISW-MRI parameters (all >30%), which is likely to reflect differences in the tumoral characteristics measured and the range of imaging techniques employed.

Individual examples of DWI and DCE-MRI responses were recorded (Supplementary Figures 3-4); however, a statistically significant cohort change in the image-derived parameters K^{trans} , ADC, or tCho/Water ratio after administration of MK-2206 was not observed (Supplementary Figure 2). These observations may be due primarily to the dose of 60mg QOD of MK-2206 being insufficient to result in alterations in vascular permeability tumor cellularity, as well as total choline and R_2^* levels that are detectable on the functional imaging undertaken; a higher MTD of 200mg QW of MK-2206 may be necessary to achieve this. Such imaging studies should thus be considered in ongoing phase II trials evaluating this dose and schedule of MK-2206. The variability in baseline measurements for the imaging parameters could also mean that the sample size was inadequate to detect small changes. Furthermore, most of the lesions selected for MRI evaluation demonstrated a slow increase in overall size during the study, indicating a lack of antitumor response to MK-2206 monotherapy and suggesting that biologically significant AKT inhibition was possibly not achieved.

In conclusion, we have used detailed safety, PK, and PD studies to establish the MTD/RP2D of MK-2206 in a QW schedule, which results in significant tumor cell target and pathway blockade while demonstrating tolerability for utility in different combination regimens.

While we have confirmed impressive AKT blockade in PD studies, we have seen little evidence of antitumor activity. This schedule of MK-2206 has now been taken forward into phase I/II trials involving both monotherapy and combination regimens in a wide range of cancers in defined patient populations [42].

Supplementary Material

Refer to Web version on PubMed Central for supplementary material.

Acknowledgments

The authors acknowledge the physicists involved in the imaging data acquisition and analysis for the trial, especially David J. Collins, Michael Germuska and Geoffrey S. Payne. The authors wish to thank Dr. Amy O. Johnson-Levonas, Martha Vollmer and Kristen Lewis (Merck & Co., Inc., Whitehouse Station, NJ, USA) for their assistance with preparing this manuscript for publication.

Acknowledgements for research support:

This study was supported by Merck & Co., Inc. The Drug Development Unit of the Royal Marsden NHS Foundation Trust and The Institute of Cancer Research is supported in part by a program grant from Cancer Research U.K. Support was also provided by the Experimental Cancer Medicine Centre (to The Institute of Cancer Research), the National Institute for Health Research (NIHR) Biomedical Research Centre (jointly to the Royal Marsden NHS Foundation Trust and The Institute of Cancer Research), the NIHR Clinical Research Facility (to the Royal Marsden NHS Foundation Trust) and the Cancer Research UK and EPSRC Cancer Imaging Centre. T.A. Yap is the recipient of the 2011 Rebecca and Nathan Milikowsky – PCF Young Investigator Award and is supported by the NIHR. M.O. Leach is an NIHR Senior Investigator.

REFERENCES

- [1]. Engelman JA. Targeting PI3K signalling in cancer: opportunities, challenges and limitations. *Nat Rev Cancer*. 2009; 9:550–62. [PubMed: 19629070]
- [2]. Yap TA, Garrett MD, Walton MI, Raynaud F, de Bono JS, Workman P. Targeting the PI3K-AKT-mTOR pathway: progress, pitfalls, and promises. *Curr Opin Pharmacol*. 2008; 8:393–412. [PubMed: 18721898]
- [3]. Jiao J, Wang S, Qiao R, Vivanco I, Watson PA, Sawyers CL, Wu H. Murine cell lines derived from Pten null prostate cancer show the critical role of PTEN in hormone refractory prostate cancer development. *Cancer Res*. 2007; 67:6083–91. [PubMed: 17616663]
- [4]. Taylor BS, Schultz N, Hieronymus H, Gopalan A, Xiao Y, Carver BS, et al. Integrative genomic profiling of human prostate cancer. *Cancer Cell*. 2010; 18:11–22. [PubMed: 20579941]
- [5]. Chen ML, Xu PZ, Peng XD, Xu C, Ruan YH, Xu ZH, et al. The deficiency of Akt1 is sufficient to suppress tumor development in Pten+/- mice. *Genes Dev*. 2006; 20:1569–74. [PubMed: 16778075]
- [6]. Yap TA, Carden CP, Kaye SB. Beyond chemotherapy: targeted therapies in ovarian cancer. *Nat Rev Cancer*. 2009; 9:167–81. [PubMed: 19238149]
- [7]. Levine DA, Bogomolny F, Yee CJ, Lash A, Barakat RR, Borgen PI, Boyd J. Frequent mutation of the PIK3CA gene in ovarian and breast cancers. *Clin Cancer Res*. 2005; 11:2875–8. [PubMed: 15837735]
- [8]. Shayesteh L, Lu Y, Kuo WL, Baldocchi R, Godfrey T, Collins C, et al. PIK3CA is implicated as an oncogene in ovarian cancer. *Nat Genet*. 1999; 21:99–102. [PubMed: 9916799]
- [9]. Cheng JQ, Godwin AK, Bellacosa A, Taguchi T, Franke TF, Hamilton TC, et al. AKT2, a putative oncogene encoding a member of a subfamily of protein-serine/threonine kinases, is amplified in human ovarian carcinomas. *Proc Natl Acad Sci U S A*. 1992; 89:9267–71. [PubMed: 1409633]
- [10]. Nakayama K, Nakayama N, Kurman RJ, Cope L, Pohl G, Samuels Y, et al. Sequence mutations and amplification of PIK3CA and AKT2 genes in purified ovarian serous neoplasms. *Cancer Biol Ther*. 2006; 5:779–85. [PubMed: 16721043]

- [11]. Courtney KD, Corcoran RB, Engelman JA. The PI3K pathway as drug target in human cancer. *J Clin Oncol.* 2010; 28:1075–83. [PubMed: 20085938]
- [12]. Bilodeau MT, Balitza AE, Hoffman JM, Manley PJ, Barnett SF, Defeo-Jones D, et al. Allosteric inhibitors of Akt1 and Akt2: a naphthyridinone with efficacy in an A2780 tumor xenograft model. *Bioorg Med Chem Lett.* 2008; 18:3178–82. [PubMed: 18479914]
- [13]. Yan, L. MK-2206: A potent oral allosteric AKT inhibitor; Presented at: AACR Annual Meeting; Denver, Col.. April 18-22, 2009; Abstract DDT01-1
- [14]. Yap TA, Yan L, Patnaik A, Fearen I, Olmos D, Papadopoulos K, et al. First-in-man clinical trial of the oral pan-AKT inhibitor MK-2206 in patients with advanced solid tumors. *J Clin Oncol.* 2011; 29:4688–95. [PubMed: 22025163]
- [15]. Tunariu N, Kaye SB, deSouza NM. Functional imaging: what evidence is there for its utility in clinical trials of targeted therapies? *Br J Cancer.* 2012; 106:619–28. [PubMed: 22281664]
- [16]. Zweifel M, Padhani AR. Perfusion MRI in the early clinical development of antivascular drugs: decorations or decision making tools? *Eur J Nucl Med Mol Imaging.* 2010; 37(Suppl 1):S164–S182. [PubMed: 20461374]
- [17]. O'Connor JP, Jackson A, Parker GJ, Jayson GC. DCE-MRI biomarkers in the clinical evaluation of antiangiogenic and vascular disrupting agents. *Br J Cancer.* 2007; 96:189–95. [PubMed: 17211479]
- [18]. Leach MO, Morgan B, Tofts PS, Buckley DL, Huang W, Horsfield MA, et al. Imaging vascular function for early stage clinical trials using dynamic contrast-enhanced magnetic resonance imaging. *Eur Radiol.* 2012; 22:1451–64. [PubMed: 22562143]
- [19]. Leach MO, Brindle KM, Evelhoch JL, Griffiths JR, Horsman MR, Jackson A, et al. The assessment of antiangiogenic and antivascular therapies in early-stage clinical trials using magnetic resonance imaging: issues and recommendations. *Br J Cancer.* 2005; 92:1599–610. [PubMed: 15870830]
- [20]. Padhani AR, Liu G, Koh DM, Chenevert TL, Thoeny HC, Takahara T, et al. Diffusion-weighted magnetic resonance imaging as a cancer biomarker: consensus and recommendations. *Neoplasia.* 2009; 11:102–25. [PubMed: 19186405]
- [21]. Padhani AR, Koh DM. Diffusion MR imaging for monitoring of treatment response. *Magn Reson Imaging Clin N Am.* 2011; 19:181–209. [PubMed: 21129641]
- [22]. Belouche-Babari M, Jackson LE, Al Saffar NM, Eccles SA, Raynaud FI, Workman P, et al. Identification of magnetic resonance detectable metabolic changes associated with inhibition of phosphoinositide 3-kinase signaling in human breast cancer cells. *Mol Cancer Ther.* 2006; 5:187–96. [PubMed: 16432178]
- [23]. Su JS, Woods SM, Ronen SM. Metabolic consequences of treatment with AKT inhibitor perifosine in breast cancer cells. *NMR Biomed.* 2012; 25:379–88. [PubMed: 22253088]
- [24]. Li SP, Taylor NJ, Makris A, Ah-See ML, Beresford MJ, Stirling JJ, et al. Primary human breast adenocarcinoma: imaging and histologic correlates of intrinsic susceptibility-weighted MR imaging before and during chemotherapy. *Radiology.* 2010; 257:643–52. [PubMed: 20858850]
- [25]. Yap TA, Omlin A, de Bono JS. Development of therapeutic combinations targeting major cancer signaling pathways. *J Clin Oncol.* 2013; 31:1592–605. [PubMed: 23509311]
- [26]. Oken MM, Creech RH, Tormey DC, Horton J, Davis TE, McFadden ET, Carbone PP. Toxicity and response criteria of the Eastern Cooperative Oncology Group. *Am J Clin Oncol.* 1982; 5:649–55. [PubMed: 7165009]
- [27]. Ji Y, Li Y, Nebiyou BB. Dose-finding in phase I clinical trials based on toxicity probability intervals. *Clin Trials.* 2007; 4:235–44. [PubMed: 17715248]
- [28]. Cancer Therapy Evaluation Program. Common Terminology Criteria for Adverse Events (CTCAE) v3.0. Bethesda, Md: 2006.
- [29]. Gowan SM, Hardcastle A, Hallsworth AE, Valenti MR, Hunter LJ, de Haven Brandon AK, et al. Application of meso scale technology for the measurement of phosphoproteins in human tumor xenografts. *Assay Drug Dev Technol.* 2007; 5:391–401. [PubMed: 17638539]
- [30]. Therasse P, Arbuck SG, Eisenhauer EA, Wanders J, Kaplan RS, Rubinstein L, et al. European Organization for Research and Treatment of Cancer; National Cancer Institute of the United

- States; National Cancer Institute of Canada. New guidelines to evaluate the response to treatment in solid tumors. *J Natl Cancer Inst.* 2000; 92:205–16. [PubMed: 10655437]
- [31]. Rustin GJ, Quinn M, Thigpen T, du Bois A, Pujade-Lauraine E, Jakobsen A, et al. New guidelines to evaluate the response to treatment in solid tumors (ovarian cancer). *J Natl Cancer Inst.* 2004; 96:487–8. [PubMed: 15026475]
- [32]. Bublely GJ, Carducci M, Dahut W, Dawson N, Daliani D, Eisenberger M, et al. Eligibility and response guidelines for phase II clinical trials in androgen-independent prostate cancer: recommendations from the Prostate-Specific Antigen Working Group. *J Clin Oncol.* 1999; 17:3461–7. [PubMed: 10550143]
- [33]. Orton MR, d’Arcy JA, Walker-Samuel S, Hawkes DJ, Atkinson D, Collins DJ, Leach MO. Computationally efficient vascular input function models for quantitative kinetic modelling using DCE-MRI. *Phys Med Biol.* 2008; 53:1225–39. [PubMed: 18296759]
- [34]. d’Arcy JA, Collins DJ, Padhani AR, Walker-Samuel S, Suckling J, Leach MO. Informatics in Radiology (infoRAD): Magnetic Resonance Imaging Workbench: analysis and visualization of dynamic contrast-enhanced MR imaging data. *Radiographics.* 2006; 26:621–32. [PubMed: 16549620]
- [35]. Banerji, U.; Ranson, M.; Schellens, JHM.; Esaki, T.; Dean, E.; Zivi, A., et al. Results of two phase I multicenter trials of AZD5363, an inhibitor of AKT1, 2 and 3: Biomarkers and early clinical evaluation in Western and Japanese patients with advanced solid tumors; Presented at: AACR Annual Meeting; Washington, DC. April 6-10, 2013; Abstract LB-66
- [36]. Bendell JC, Rodon J, Burris HA, de Jonge M, Verweij J, Birtle D, et al. Phase I, dose-escalation study of BKM120, an oral pan-Class I PI3K inhibitor, in patients with advanced solid tumors. *J Clin Oncol.* 2012; 30:282–90. [PubMed: 22162589]
- [37]. Burris, HA.; Siu, LL.; Infante, JR.; Wheler, JJ.; Kurkjian, C.; Opalinska, J., et al. Safety, pharmacokinetics (PK), pharmacodynamics (PD), and clinical activity of the oral AKT inhibitor GSK2141795 (GSK795) in a phase 1 first-in-human study; Presented at: ASCO Annual Meeting; Chicago, Ill.. June 3-7, 2011; Abstract 3003
- [38]. Tabernero, J.; Saura, C.; Roda Perez, D.; Dienstmann, R.; Rosello, S.; Prudkin, L., et al. First-in-human phase I study evaluating the safety, pharmacokinetics (PK), and intratumor pharmacodynamics (PD) of the novel, oral, ATP-competitive Aky inhibitor GDC-0068; Presented at: ASCO Annual Meeting; Chicago, Ill.. June 3-7, 2011; Abstract 3022
- [39]. Crouthamel MC, Kahana JA, Korenchuk S, Zhang SY, Sundaresan G, Eberwein DJ, et al. Mechanism and management of AKT inhibitor-induced hyperglycemia. *Clin Cancer Res.* 2009; 15:217–25. [PubMed: 19118049]
- [40]. Yan Y, Serra V, Prudkin L, Scaltriti M, Murli S, Rodriguez O, et al. Evaluation and Clinical Analyses of Downstream Targets of the Akt Inhibitor GDC-0068. *Clin Cancer Res.* 2013; 19:6976–86. [PubMed: 24141624]
- [41]. Tolcher, AW.; Baird, RD.; Patnaik, A.; Moreno Garcia, V.; Papadopoulos, KP.; Garret, CR., et al. A phase I dose-escalation study of oral MK-2206 (allosteric AKT inhibitor) with oral selumetinib (AZD6244; MEK inhibitor) in patients with advanced or metastatic solid tumors; Presented at: ASCO Annual Meeting; Chicago, IL. June 3-7, 2011; Abstract 3004
- [42]. National Institutes of Health (NIH). NIH; Bethesda, Md: [cited 2014]. Available from: <http://www.clinicaltrials.gov>

STATEMENT OF TRANSLATIONAL RELEVANCE

MK-2206 is a novel, specific, oral inhibitor of AKT, which is deregulated in multiple cancers. The study of different schedules of targeted agents is critical for their optimal application. The maximum tolerated dose (MTD) of MK-2206 was previously established at 60mg on alternate days (QOD). Due to a long half-life of 60h-80h, MK-2206 was evaluated in a weekly schedule for comparison with QOD dosing in this study. The MK-2206 weekly schedule appeared to be similarly tolerated to QOD dosing, while pharmacodynamic studies using novel quantitative electrochemiluminescence assays in serially-obtained tumor and platelet-rich plasma (PRP) specimens confirmed significant AKT blockade with both continuous QOD and intermittent schedules of MK-2206. Functional imaging studies demonstrated that complex multiparametric MRI protocols may be effectively implemented in phase I trials. The intermittent weekly MTD of 200mg of MK-2206 established in this study is currently used in multiple phase II monotherapy and combination studies in defined patient populations.

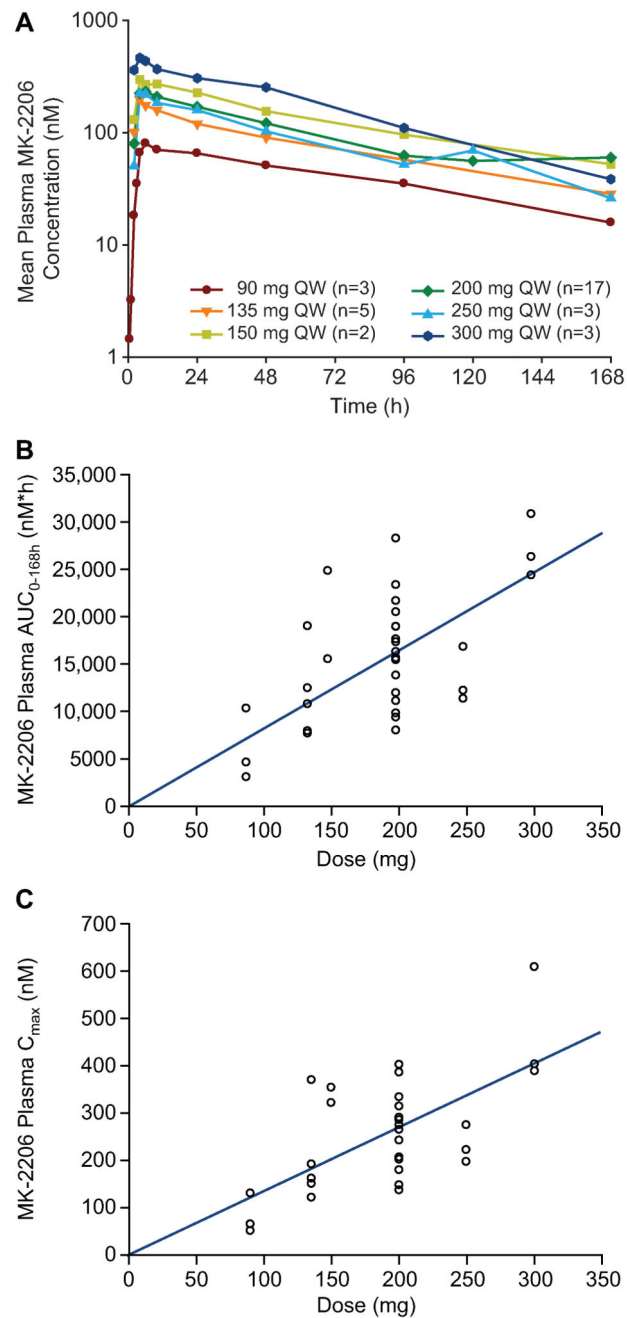


Figure 1. Pharmacokinetic profile of MK-2206 in QW schedule

A: Mean plasma MK-2206 concentrations (nM) following the first dose of Cycle 1.

B: MK-2206 plasma AUC_{0-168hr} (nM*hr) following the first dose of Cycle 1.

C: MK-2206 plasma C_{max} (nM) following the first dose of Cycle 1.

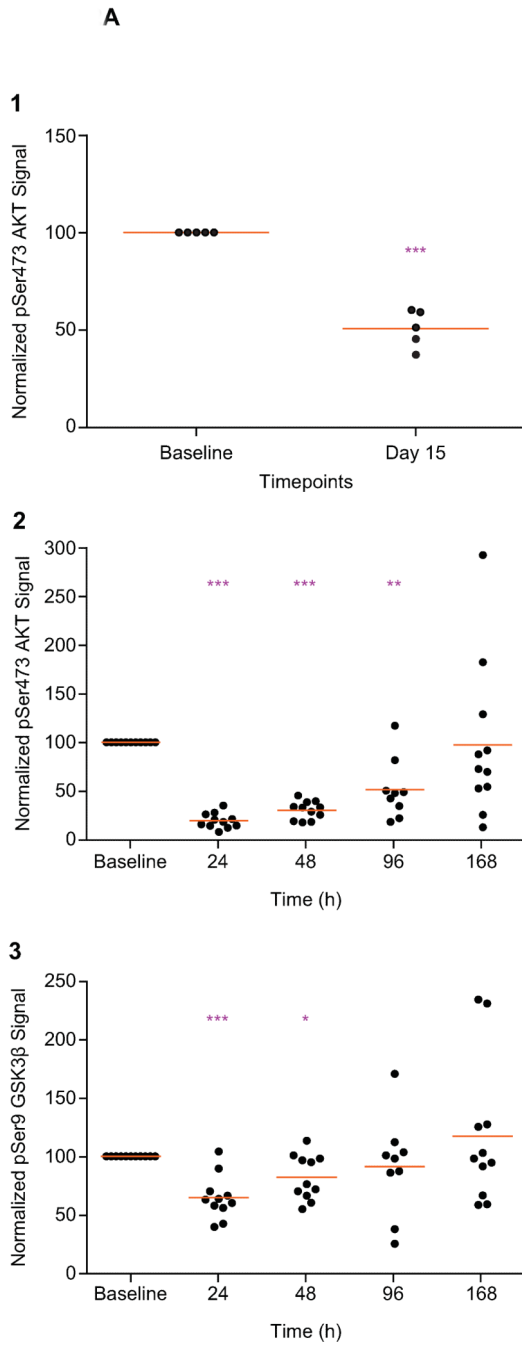


Figure 2A. Pharmacodynamic profile of MK-2206 in tumor and platelet-rich plasma (PRP) in a QW schedule

The analysis of paired tumor biopsies from 5 patients receiving 200mg QW of MK-2206 (**Figure 2A1**) showed a significant suppression of pSer473 AKT, when compared with paired pre-treatment samples. Overall, the pSer473 AKT signal decreased to 50.0% (range 37.5-60.3%; $p=0.0003$) of baseline levels on MK-2206 treatment, confirming target modulation. The PD effects of MK-2206 treatment on pSer473 AKT ($n=11$) and pSer9 GSK3 β ($n=11$) phosphorylation at the 200mg MTD were also assessed sequentially in PRP

specimens at multiple timepoints (**Figures 2A2 – 2A3**). The mean pSer473 AKT signal post-MK-2206 was 19.8% at 24h ($p<0.0001$), 30.6% at 48h ($p<0.0001$), 51.7% at 96h ($p=0.0015$) and 97.4% at 168h ($p=0.92$) of baseline levels (**Figure 2A2**), while mean pSer9 GSK3 β signal was 65.0% at 24h ($p<0.0001$), 82.3% at 48h ($p=0.012$), 91.4% at 96h ($p=0.56$) and 117.2% at 168h ($p=0.37$) of baseline levels (**Figure 2A3**). * $p<0.05$; ** $p<0.01$; *** $p<0.001$ Paired t test compared to baseline. Points represent the levels of PD biomarkers as a percent of the baseline levels for individual patients and orange lines represent mean of all patients at that time point.

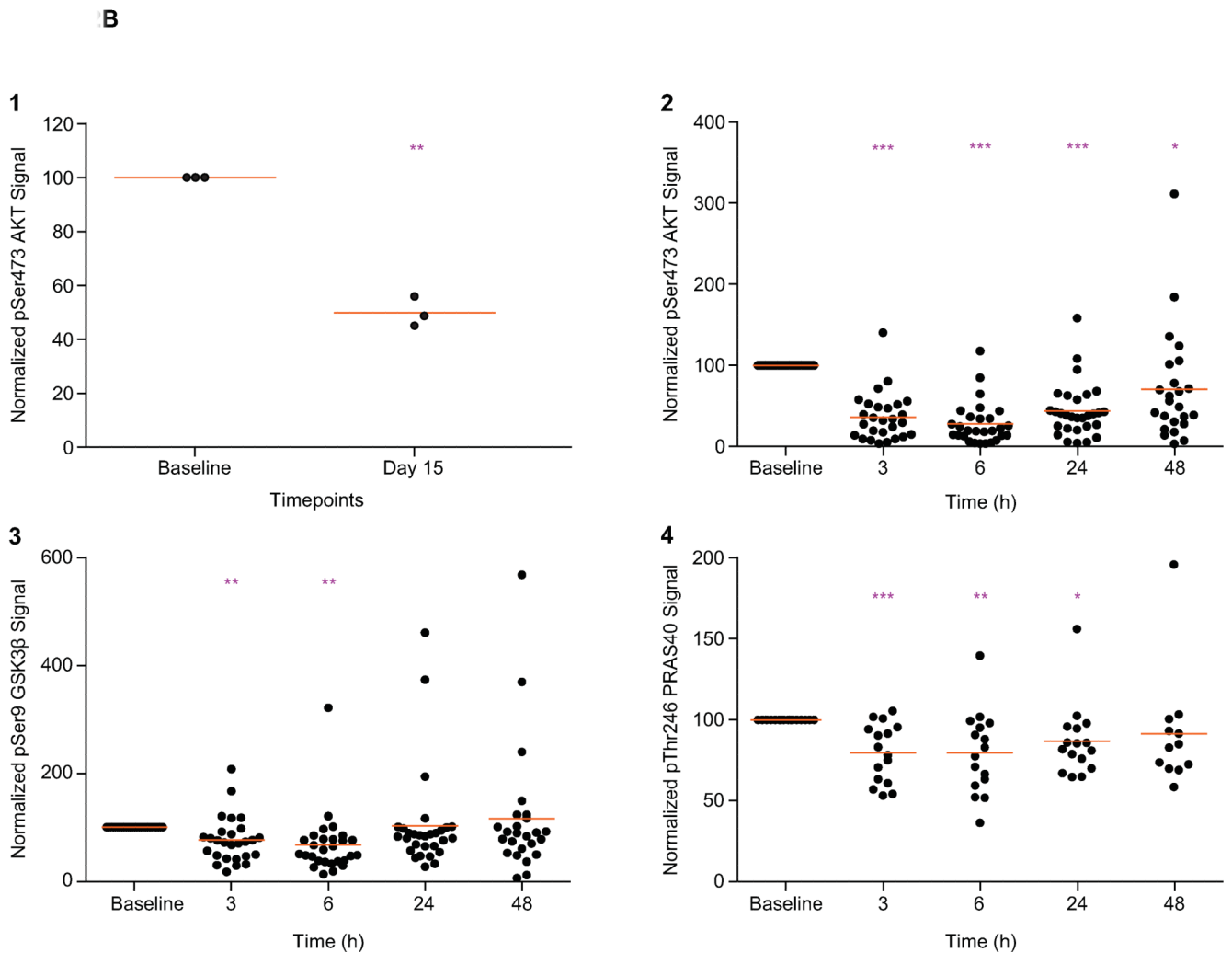


Figure 2B. Pharmacodynamic profile of MK-2206 in platelet-rich plasma (PRP) and tumor in a QOD schedule

Paired tumor biopsies were also obtained for biomarker analysis by MSD[®] electrochemiluminescence assays from 3 patients receiving 60mg QOD of MK-2206. All 3 patients showed a significant suppression of pSer473 AKT, when compared with paired pre-treatment samples (**Figure 2B1**). The mean pSer473 AKT levels decreased to 50.1% (range 45.3-56.2%; $p=0.004$) of baseline levels on MK-2206 treatment, confirming target modulation. PD effects in PRP were also assessed serially at multiple timepoints from 29 patients receiving the MTD of 60mg QOD of MK-2206 (**Figures 2B1-2B4**). The pSer473 AKT signal decreased significantly to mean of 36.3% at 3h ($p<0.0001$), 27.9% at 6h ($p<0.0001$), 44.0% at 24h ($p<0.0001$) and 70.6% at 48h ($p=0.045$) of baseline levels (**Figure 2B2**). Inhibition of pSer473 AKT was associated with significant decreases in the phosphorylation of downstream substrates pSer9 GSK3 β to mean levels of 76.8% at 3h ($p=0.009$), 67.5% at 6h ($p=0.0051$), 102.9% at 24h ($p=0.87$) and 9116.1% at 48h ($p=0.51$) of baseline levels (**Figure 2B3**); and pThr246 PRAS40 to mean levels of 79.8% at 3h ($p=0.005$), 79.7% at 6h ($p=0.0059$), 86.9% at 24h ($p=0.030$) and 91.4% at 48h ($p=0.42$) of baseline levels (**Figure 2B4**). * $p<0.05$; ** $p<0.01$; *** $p<0.001$ Paired t-test compared to

baseline. Points represent the levels of PD biomarkers as a percent of the baseline levels for individual patients and orange lines represent mean of all patients at that timepoint.

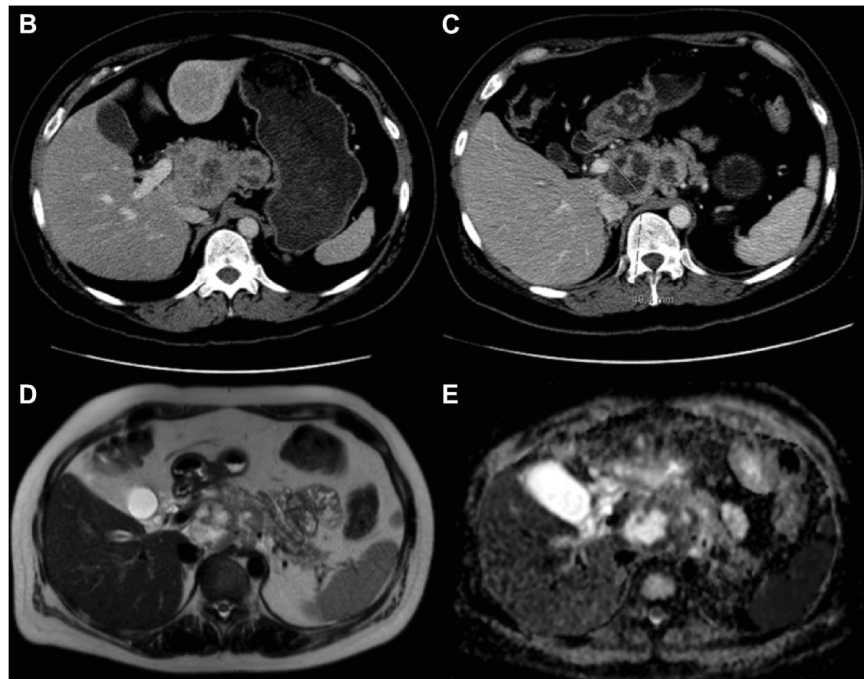
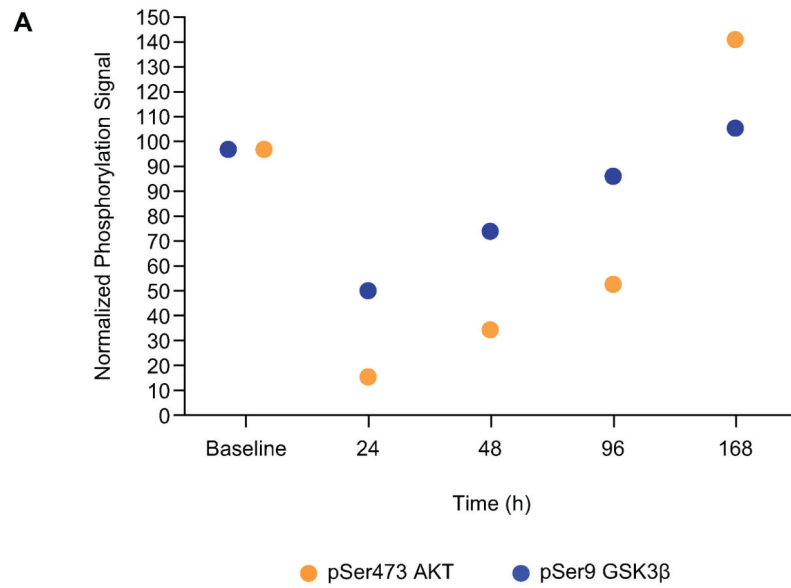


Figure 3. Best responder

A 43-year-old female with ER/PR positive, HER2 negative metastatic breast cancer treated with 150mg QW of MK-2206. PD studies demonstrated maximal suppression of pSer473 AKT and its substrate pSer9 GSK3β at 24h, followed by a gradual recovery of phosphorylation signals from 48h in PRP. Points represent the levels of PD biomarkers as a percent of the baseline levels (A). Molecular characterization of circulating nucleic acids demonstrated a *PIK3CA* exon 20 mutation and low Ki67 proliferation. The patient had previously received treatments including cyclophosphamide, doxorubicin and radiotherapy.

Following 8 weeks of treatment with MK-2206 150mg QW, there was a 22% reduction in RECIST measurements of her target lesions in the liver metastases, celiac axis and para-aortic lymph nodes (**B-C**). Post treatment MRI demonstrated intratumoral necrosis in liver and bone lesions, as evidence by the high signal on anatomical T2 weighted images (**D**), and the high ADC values on DWI-MRI (overall lymph node mass ADC was $170 \times 10^{-5} \text{ mm}^2/\text{s}$; the mean ADC in the areas of necrosis was greater than $200 \times 10^{-5} \text{ mm}^2/\text{s}$) (**E**). Consistent with these findings, CA15-3 levels decreased by 36% (6853U/ml to 4399U/ml) and the patient remained on treatment for a total of 24 weeks before developing disease progression.

Table 1

Patient baseline characteristics – all treated patients (N=71)

60mg QOD schedule N=38	n (%)	QW schedule N=33	n (%)
Sex		Sex	
Male	20 (52.6)	Male	18 (54.5)
Female	18 (47.4)	Female	15 (45.5)
Median age, years (range)	63 (39-75)	Median age, years (range)	59 (32-75)
Cancer type		Cancer type	
Prostate	15	Prostate	7
Colon/rectum	5	Colon/rectum	7
Breast	1	Breast	6
Ovarian	12	Ovarian	2
Renal cell	3	Mesothelioma	2
Other ^a	2	Other ^b	9
ECOG PS at screening		ECOG PS at screening	
0	9	0	13
1	29	1	20
All prior therapies ^c		All prior therapies ^c	
1-2	8	1-2	13
>2	30	>2	20

^aIncludes bile duct carcinoma and leiomyosarcoma (n=1 each)

^bIncludes bronchial carcinoma, leiomyosarcoma, melanoma, neuroendocrine tumor, pancreatic carcinoma, renal cell carcinoma, urothelial carcinoma, uterine carcinoma, and unknown primary carcinoma (all n=1)

^cIncludes chemotherapy, radiotherapy, hormone therapy and immunotherapies

Table 2

Treatment-related adverse events (AEs) for the QW dosing cohort. All values shown are the number of AEs occurring in n 2 during cycle 1, and all cycles (parentheses)

Cohort	Common Treatment-Related Adverse Events ^a													
	90mg (n=3)	135mg (n=5)	150mg (n=2)			200mg (n=17)			250mg (n=3)			300mg (n=3)		
AE	G1	G1	G1	G2	G3	G1	G2	G3	G1	G2	G3	G1	G2	G3
Gastrointestinal disorders														
Diarrhea	1 (1)	0 (0)	0 (0)	0 (0)	0 (0)	2 (2)	0 (0)	0 (0)	0 (0)	0 (0)	0 (0)	0 (0)	0 (0)	0 (0)
Nausea	0 (0)	0 (0)	0 (0)	1 (1)	0 (0)	4 (4)	1 (1)	0 (0)	0 (0)	0 (0)	0 (0)	1 (1)	0 (0)	0 (0)
Stomatitis	0 (0)	0 (0)	0 (0)	0 (0)	0 (0)	2 (2)	0 (0)	0 (0)	1 (2)	0 (0)	0 (0)	0 (0)	1 (1)	0 (0)
Vomiting	1 (1)	0 (0)	2 (2)	0 (0)	0 (0)	2 (2)	0 (0)	0 (0)	0 (0)	0 (0)	0 (0)	0 (0)	0 (0)	0 (0)
General disorders														
Fatigue	1 (1)	0 (0)	0 (0)	0 (0)	0 (0)	0 (2)	1 (1)	0 (0)	0 (0)	0 (0)	0 (0)	1 (1)	0 (0)	0 (0)
Metabolism and nutrition disorders														
Anorexia	0 (0)	0 (0)	0 (1)	0 (0)	0 (0)	1 (1)	0 (0)	0 (0)	0 (0)	0 (0)	0 (0)	0 (0)	0 (0)	0 (0)
Nervous system disorders														
Dysgeusia	0 (1)	0 (0)	0 (0)	0 (0)	0 (0)	0 (0)	0 (0)	0 (0)	0 (0)	0 (0)	0 (0)	1 (1)	0 (0)	0 (0)
Skin and subcutaneous tissue disorders														
Dermatitis acneiform	0 (0)	1 (1)	0 (0)	0 (0)	0 (0)	0 (0)	0 (0)	0 (0)	1 ^c (1)	0 (0)	0 (0)	0 (0)	0 (0)	0 (0)
Dry skin	0 (0)	0 (0)	0 (0)	0 (0)	0 (0)	1 (1)	0 (0)	0 (0)	0 (0)	0 (0)	0 (0)	0 (0)	0 (0)	0 (0)
Pruritus	0 (0)	1 (1)	0 (0)	0 (0)	0 (0)	0 (2)	0 (1)	0 (0)	0 (0)	0 (0)	0 (0)	0 (0)	0 (0)	0 (0)
Rash ^b	0 (0)	1 (1)	0 (0)	0 (0)	1 ^c (3)	5 (9)	4 (4)	3 ^c (3)	0 (1)	1 (2)	2 ^c (2)	5 (6)	2 (2)	3 ^c (3)

No treatment-related G4-5 AEs were observed during the study.

No treatment-related G2, 3 or 4 AEs were observed in the 90mg or 135mg dose cohorts.

^a All values shown represent number of AEs occurring in 2 patients during first cycle, and all cycles (parentheses). If a patient experienced the same AE multiple times (at the same or different grade), the adverse event counted every time it occurred.

^b All preferred AE terms with "rash" (e.g. rash macular, rash papular, etc.) were collated into the single term of "Rash".

^c Dose-limiting toxicity.

TABLE 3
 MK-2206 Protocol 002 Preliminary Results: Summary PK Parameter Values Following Multiple QW Doses of 90, 135, 150, 200, 250 and 300mg of MK-2206 in Male and Female Oncology Patients

QW Dose (mg)	N (Day 1, Day last)	AUC _{0-168h} (nmol × h/L) Mean ± SD (%CV)			C _{max} (nmol/L) Mean ± SD (%CV)			C _{48h} (nmol/L) Mean ± SD			T _{max} (h) ^d		Apparent Terminal t _{1/2} ^b (h)
		Day 1	Last Day	Last Day / Day1 Ratio ^c	Day 1	Last Day	Last Day / Day1 Ratio ^c	Day 1	Last Day	Last Day / Day1 Ratio ^c	Day 1	Last Day	
90	3, 3	6510 ± 3810 (59%)	10600 ± 7520 (71%)	<i>d</i>	81.7 ± 42.4 (52%)	153 ± 98.0 (64%)	<i>d</i>	50.9 ± 38.2	79.3 ± 33.7	1.61	6.0 (4.0-10.0)	4.0 (4.0-4.0)	71.6 ± 12.2
135	5, 4	12000 ± 4610 (38%)	20700 ± 8780 (42%)	1.91	199 ± 98.9 (50%)	352 ± 210 (60%)	1.95	90.3 ± 25.1	158 ± 59.2	1.86	4.0 (4.0-10.0)	5.0 (4.0-24.0)	88.9 ± 26.9
150	2, 1	20700	22600	<i>d</i>	337	346	<i>d</i>	155	185	<i>d</i>	(4.0-10.0)	4.0	64.4
200	17, 13	16400 ± 5470 (33%)	23500 ± 14700 (63%)	1.54	264 ± 75.8 (29%)	345 ± 199 (58%)	1.33	121 ± 47.4	187 ± 113	1.49	6.0 (4.0-10.0)	6.0 (4.0-24.0)	75.1 ± 14.7
250	3, 1	14000 ± 2950 (21%)	10700	<i>d</i>	231 ± 39.1 (17%)	169	<i>d</i>	103 ± 19.6	74.8	<i>d</i>	6.0 (4.0-6.0)	4.0	53.7
300	3, 0	27700 ± 3320 (12%)	<i>d</i>	<i>d</i>	466 ± 123 (26%)	<i>d</i>	<i>d</i>	253	<i>d</i>	<i>d</i>	4.0 (4.0-6.0)	<i>d</i>	<i>d</i>

Abbreviations: AUC, area under the concentration-time curve; C_{max}: maximum measured plasma concentration; C_{48hr}: plasma concentration 48 hours following dose (trough concentration); T_{max}: time from dosing to maximum plasma concentration; t_{1/2}: half-life; SD, standard deviation

^aMedian (min - max)

^bHarmonic mean ± pseudo SD

^cGeometric mean

^dSummary statistics not provided due to insufficient data